Electronic Supplementary Information (ESI)

Assessment of the zero-valent iron-based nanotherapeutics for ferroptosis induction and resensitization strategy in cancer cells

Kuang-Jing Huang,[a] Yau-Huei Wei,[b] Yen-Chi Chiu,[a] Shang-Rung Wu,[*a,c] Dar-Bin Shieh[*a,c,d,e,f]

[a]Institute of Basic Medical Sciences, College of Medicine, National Cheng Kung University, Tainan 70101, Taiwan

[b]Center for Mitochondrial Medicine and Free Radical Research, Changhua Christian Hospital, Changhua 50006, Taiwan

[c]Institute of Oral Medicine, College of Medicine, National Cheng Kung University, Tainan 70101, Taiwan

[d]Institute of Clinical Medicine, College of Medicine, National Cheng Kung University College of Medicine and Hospital, Tainan 70101, Taiwan

[e]Center of Applied Nanomedicine, Center for Micro/Nano Science and Technology, Advanced Optoelectronic Technology Center, Innovation Center for Advanced Medical Device Technology, National Cheng Kung University, Tainan 70101, Taiwan

[f]Department of Stomatology, National Cheng Kung University Hospital, Tainan 70101, Taiwan

*Correspondence to: dbshieh@mail.ncku.edu.tw (D.B. Shieh); shangrungwu@gmail.com (S.R Wu)

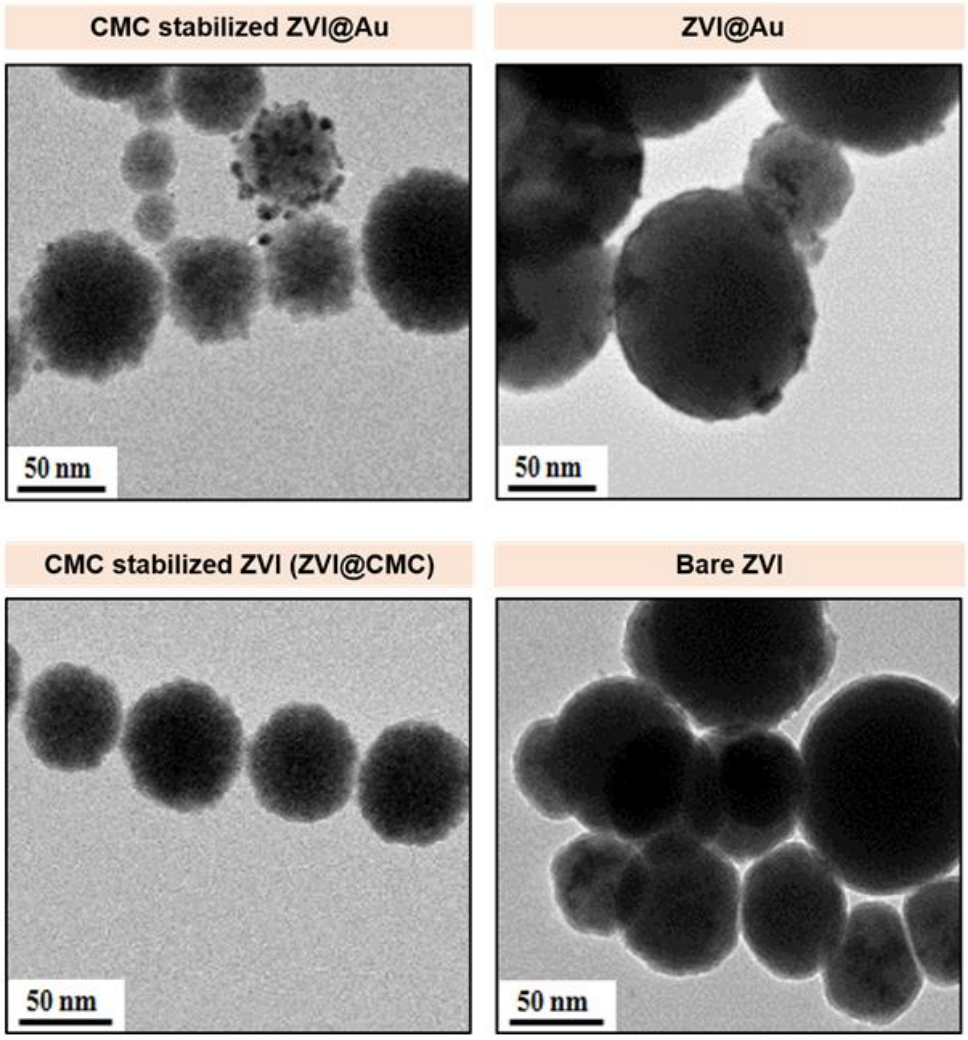

Fig. S1 Characterization of the ultrastructure of different ZVI-based nanoparticles by TEM. TEM images show that all the synthesized NPs used in the experiment had a diameter in the range of 50 to 100 nm. Strong aggregation by the bare ZVI NPs was noted. Gold and CMC coating significantly decrease particle aggregation.

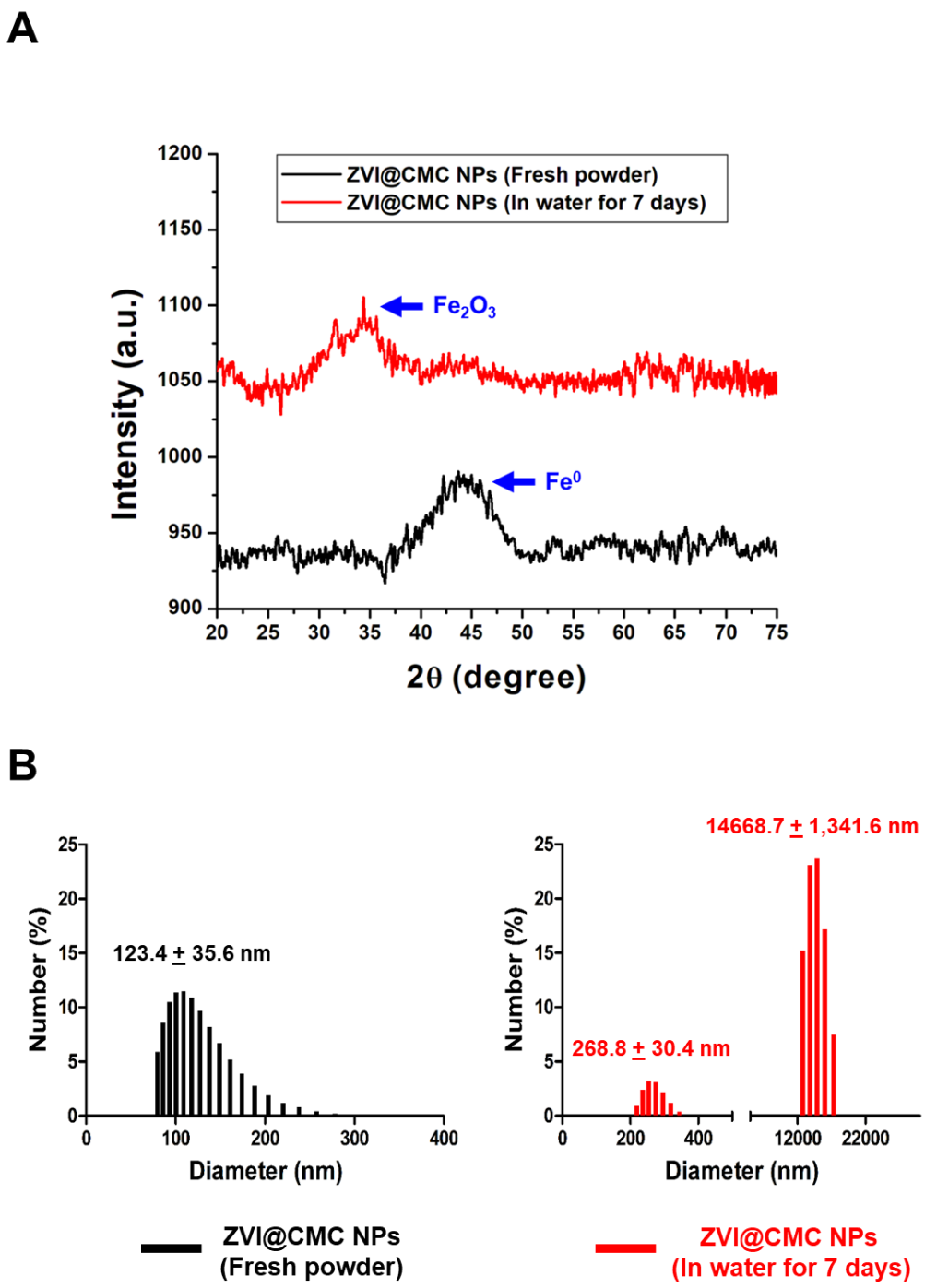

Fig. S2 Characterization of fresh prepared and oxidized ZVI@CMC NPs by XRD and DLS analysis. (A) The freshly prepared ZVI@CMC NPs presented major XRD peak at 2θ = 44.67 corresponding to that of the standard Fe^0 supporting ZVI to be the main component of the NPs. However, the shift of the XRD peak to 2θ =35.63 (iron oxide signal) was discovered in the oxidized NPs. (B) Hydrodynamic size and aggregation were increase in oxidized ZVI NPs.

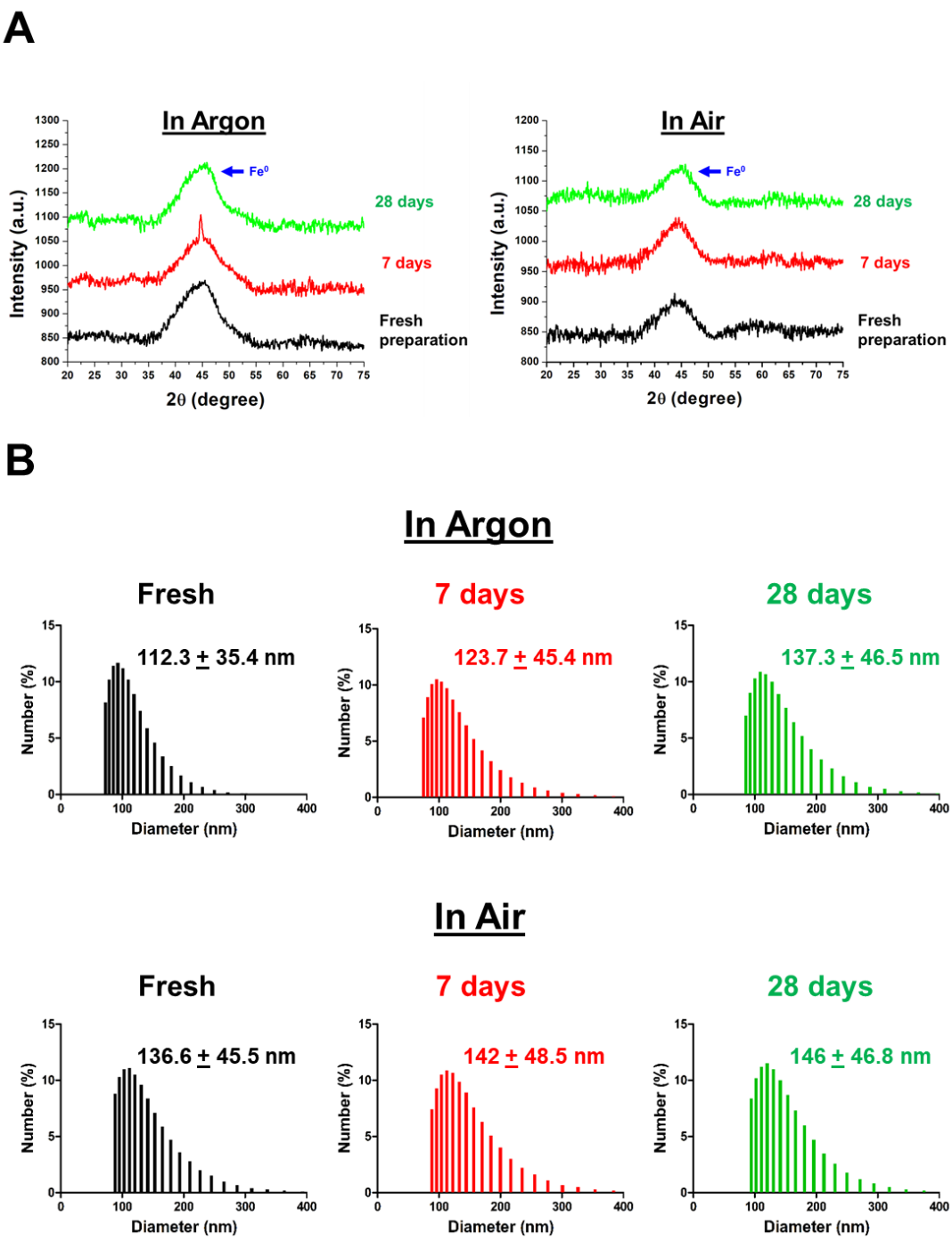

Fig. S3 Characterization of ZVI@CMC NPs in different storage condition for a period of time by XRD and DLS analysis. (A) These NPs were discovered to be quite stable when preserved in Argon or air up to 28 days even at room temperature as evidenced by well-preserved Fe^0 signal. (B) There are no significant differences in hydrodynamic size change of ZVI@CMC NPs under Argon or air environment.

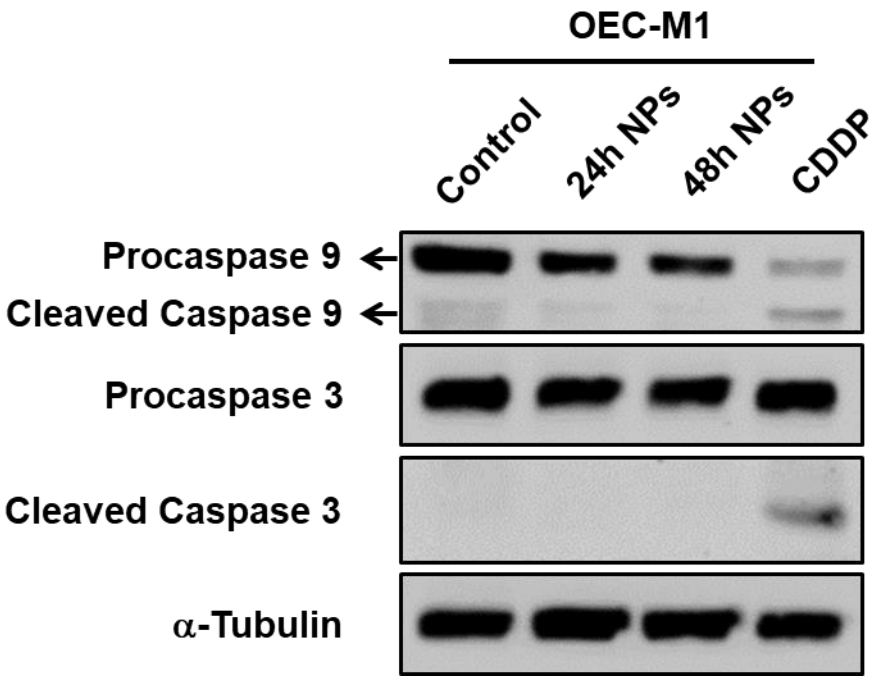

Fig. S4 Caspase-dependent apoptosis was not detected in OEC-M1 cells after ZVI NPs treatment. Western blotting revealed that the cleaved caspase 3 and caspase 9 were not detected 24 and 48 h after 5 μg/mL ZVI NP treatment. Cisplatin (CDDP, 20 μM) treatment served as a positive control.

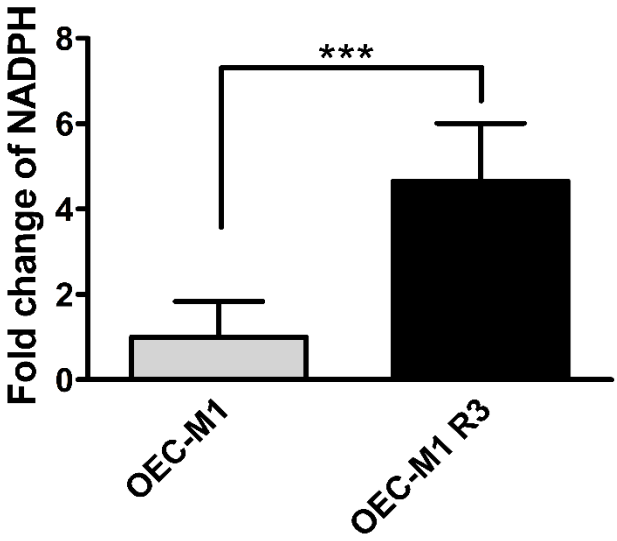

Fig. S5 Assessment of NADPH levels paired ZVI-sensitive/resistant cells. The ZVI-refractory cell line OEC-M1 R3 had much higher endogenous NADPH levels than the paired sensitive line OEC-M1.

Table S1. The IC_{50} of seven OSCC cell lines to four ZVI-based NPs.

		IC_{50} (μg/mL)			
		Bare ZVI NPs	ZVI@Au NPs	CMC stabilized ZVI@Au NPs	ZVI@CMC NPs
Sensitive cells	OC3	0.60 ± 0.02	3.48 ± 0.03	0.58 ± 0.01	0.63 ± 0.01
	OEC-M1	1.09 ± 0.15	1.48 ± 0.06	4.58 ± 0.38	4.88 ± 0.80
	SCC9	0.80 ± 0.12	7.05 ± 2.73	0.66 ± 0.01	0.76 ± 0.02
Refractory cells	HSC-3	> 50	> 50	> 50	> 50
	SAS	> 50	> 50	> 50	> 50
	KOSC-3	> 50	> 50	> 50	> 50
	OC2	> 50	> 50	> 50	> 50

Table S2. Sequences of the primers used for qPCR analysis

	Primer sequence	
Gene	**Forward**	**Reverse**
ACSL4	**GCTATCTCCTCAGACACACCGA**	**AGGTGCTCCAACTCTGCCAGTA**
ZEB1	**GCCAATAAGCAAACGATTCTG**	**TTTGGCTGGATCACTTTCAAG**
GSR	**AACATCCCAACTGTGGTCTTCAGC**	**TTGGTAACTGCGTGATACATCGGG**
AKR1C1	**AGTAAAGCTTTAGAGGCCAC**	**CACCCATGGTTCTTCTCGG**
AKR1C3	**GGGATCAACGAGAGACAAACG**	**AAAGGACTGGGTCCTCCAAGA**
AKR1B1	**TGAGTGCCACCCATATCTCA**	**TGTCACAGACTTGGGGATCA**
AKR1B10	**GTGGGGGAAGCCATCCAAGA**	**CAGCTTCAGGTCCTTGAGGG**
KYNU	**TTGCCTGCTGGTGTTCCTAC**	**TCATGAATGAAGGCACCAGC**
NNMT	**GAATCAGGCTTCACCTCCAA**	**TCACACCGTCTAGGCAGAAT**
GPx-4	**GCCTTCCCGTGTAACCAGT**	**GCGAACTCTTTGATCTCTTCGT**